García-Ruiz, A., Martins, H. F., Magalhães, R., Pereira, J. M. B., Tarasenko, O., Norin, L., Margulis, W., Martín-López, S. & González-Herráez, M. 2019, "Hermetic carbon coatings for electro-thermal all-fiber phase modulators", JLT, vol. 37, no. 18, pp. 4567-4572

Available at http://dx.doi.org/10.1109/JLT.2019.2911426

(Article begins on next page)

Hermetic carbon coatings for electro-thermal all-fiber phase modulators

Andres Garcia-Ruiz, Hugo F. Martins, Regina Magalhães, João M. B. Pereira, Oleksandr Tarasenko, Lars Norin, Walter Margulis, Sonia Martin-Lopez, Miguel Gonzalez-Herraez

***Abstract*—Joule effect and thermal response of several carbon-coated fibers are modelled and analysed. An electro-thermally driven all-fiber phase modulator based on these principles is proposed and a proof of concept of it is characterized. This kind of fibers could be the basis for developing all-fiber components aimed to operate in environments where the strength increase and impermeability to hydrogen diffusion guaranteed by the carbon coating is crucial.**

***Index Terms*—Carbon, Electrothermal effects, Optical fiber protective covering, Optical time domain reflectometry, Phase modulation, Rayleigh scattering,**

I. Introduction

OPTICAL fiber hermetic coatings play an important role in a great diversity of fiber systems, but they can be fundamental regarding fiber optic sensing systems. Many of the usual environments of fiber-optic sensors turn out to be extremely harsh, particularly in industries such as oil and gas extraction and transport [1], or even non-invasive surgery [2]. This kind of scenario is characterized by a wide range of temperature and/or pressure, plus an elevated water concentration in the atmosphere, to which the fiber is exposed. Hermetic coatings are in these cases indispensable, since they offer complete impermeability to water and hydrogen. A thin but hermetic barrier is able to protect the fiber against the diffusion of small molecules into the glass, which would otherwise derive in optical loss and strength reduction due to fatigue [3]. For these reasons, whenever a fiber system is required to operate in harsh environments where extreme records of temperature and humidity can be reached, a hermetic coating is considered. This has implications for all the elements comprised in such a fiber optics system, highlighting the relevance of making hermetic-coated all-fiber devices available.

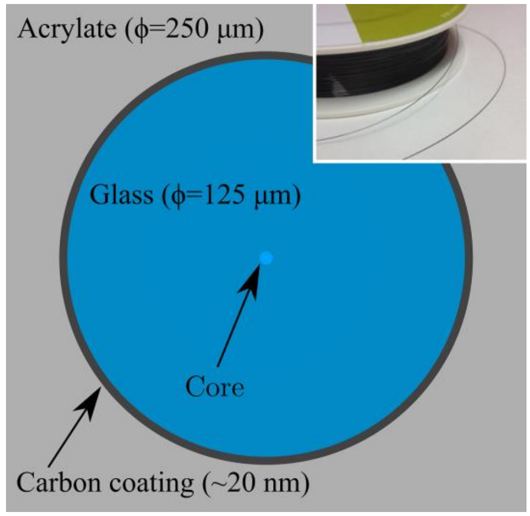

Fig. 1. Diagram of the cross section of the employed carbon-coated fibers (dimensions not to scale). The inset photograph shows one of them coiled in a spool.

Among all the possible materials, carbon represents one of the most successful choices when a hermetic fiber coating is required. Some of the most demanding contexts for sensing applications, for example the avionics industry, cannot indeed afford employing alternatives such as metallic coatings. As with carbon, these coatings can be applied during the fiber-draw process (allowing for long fiber runs to be manufactured). However, a metallic coating would imply much more weight and a poorer miniaturization of the system, due to the optical loss that small bending radii would cause in those fibers. In addition, electrical conductivity is an interesting property for a fiber coating in the field of sensing, and it has been useful to develop chemical sensors [4], or wind speed sensors [6], while it has also a central role in our study. The black coating illustrated in Fig. 1, has additional optical properties that can be exploited. For instance, it effectively isolates blue light propagating in the glass fiber from reaching the polymer coating where it could excite fluorescence and disturb sensitive

Manuscript submitted January, 2019. This work was supported by the ERC through project U-FINE (gr. 307441); the EC H2020 and Spanish MINECO (project DOMINO, ERANET Cofund Water Works 2014 call); the FINESSE project MSCA-ITN-ETN-722509; the MINECO (project TEC2015-71127-C2-2-R and a “Ramón y Cajal” contract); the regional program SINFOTON-CM: S2013/MIT-2790; and the University of Alcalá (FPI contract).

A. Garcia-Ruiz, H. F. Martins, Regina Magalhães, S. Martin-Lopez and M. Gonzalez-Herraez are with the Department of Electronics, University of Alcalá, 28805, Alcalá de Henares (Madrid), Spain (e-mail: andres.garciaruiz@uah.es; h.fidalgo@uah.es; regina.teixeira@uah.es; sonia.martinlo@uah.es; miguel.gonzalezh@uah.es).

J. M. B. Pereira, Oleksandr Tarasenko, Lars Norin, and W. Margulis are with the Department of Fiber Photonics, RISE Acreo AB, Electrum 236, 16440, Kista, Sweden (e-mail: joao.pereira@ri.se; oleksandr.tarasenko@ri.se; lars.norin@ri.se; walter.margulis@ri.se). J. M. B. Pereira and W. Margulis are also with the Department of Applied Physics, Royal Institute of Technology, Roslagstullsbacken 21, 10691 Stockholm, Sweden.

Raman signal detection [7].

In this work, we demonstrate that the thin carbon film can heat the fiber when current flows through it. We report that the fiber can reach temperatures well above 100ºC and we present a study of the electrical behavior and the dynamics of the heating process. This opens a possibility for making meter-long fiber phase controllers that are electrically-driven, starting from spools drawn in kilometer lengths: thanks to a small current applied on the carbon coating of a section of the optical fiber, it is possible to modify the refractive index (*n*) of its core in a controlled manner due to the temperature increase caused by Joule effect.

To test the dynamic response and reliability of this effect as a proof of concept of the proposed modulator, a chirped-pulse phase-sensitive optical time-domain reflectometry interrogator (CP-ΦOTDR) was used to provide high repetition rate measurements of the refractive index variations at the fiber core. This monitoring scheme has already proven high-sensitivity and dynamic (acoustic) performance in strain and temperature measurements [6], which makes it a suitable instrument for this characterization. We support the experimental results by including numerical simulations of the heating process.

II. Experimental principles and setup

Pieces of fiber of 125 µm outer diameter (see Fig. 1) and coated with a ~20 nm-thick carbon layer have been used in the experiments, both single-mode and multimode (50 µm and 62.5 µm core). This thickness was estimated from transmission electron microscopy measurements. The coating had an electrical resistance in the range from 6.3 kΩ/cm to 3.7 kΩ/cm in the highest conductivity sample, the variation arising primarily from resistivity change from fiber to fiber [8]. The deposition of the thin carbon layer on the fiber cladding surface was performed by chemical vapor deposition from a hydrocarbon gas during the fiber drawing procedure at 1850ºC. The carbon was protected with a standard external acrylate coating with a thickness of ~63 µm. Silver epoxy is used to contact the fiber to wires (Fig. 2). Optically and mechanically, the fibers behave as standard fibers. Current produced with 220 V AC bias and with high voltage DC rectification (up to 2.2 kV) was used for heating. The temperature reached by the fibers heated electrically was determined with a commercial distributed temperature sensor (DTS) based on Raman scattering with resolution 1 K and 1 m. For the experimental measurements of the dynamic response, smaller currents were needed, because of the high sensitivity of the CP-ΦOTDR method.

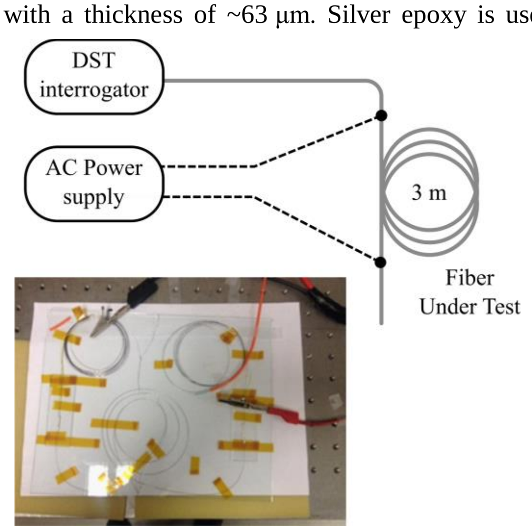

Fig. 2. Scheme and photograph of the typical C-coated fiber setup during the experiments.

For all the experiments, the fiber was placed on the top of an optical table, being surrounded mainly by *room-temperature* air. Thus, if we consider that all the power is being convectively dissipated and assume a steady state has been reached, the temperature difference with the non-excited state (T_o) is given by the *Newton's law of cooling* [9]:

$$P = h\,S\,(T - T_o), \tag{1}$$

where P is the power being dissipated by the heated body, S is the area of its external surface, and the factor h accounts for the efficiency of the convective process. This parameter usually ranges from 2 to 25 W/(m^2 K) for free convection in gases [8]. However, h has a strong dependence on the geometry of the system, as well as on the viscosity, heat capacity or flowing speed of the fluid that surrounds the body. Some of these dependencies can be derived and semi-empirical formulas exist, allowing for more realistic modeling of the system.

The direct integration of equation (1) leads to an exponential temperature evolution in time with amplitude *A*:

$$T(t) - T_o = A\,e^{-t/\tau}. \tag{2}$$

In this model, the time constant τ is determined by the effective heat capacity (C^{eff}) of the fiber, the area of its external surface (*S*), and the convective efficiency *h*:

$$\tau = \frac{C^{\text{eff}}}{h\,S}. \tag{3}$$

It represents the ratio between the stored and the dissipated portions of thermal energy. Note that a system with a small effective heat capacity will spend less time storing the injected energy before it reaches the equilibrium temperature (*T*) established by equation (1). If the system and the fluid around it, in addition, provide a high value of h, the rapid convective loss will imply a smaller difference $(T - T_o)$, implying a low characteristic time.

A rough estimation of the temperature range to be expected for a certain value of P can be done considering Eq. 1. Assuming a value of h~15 W/(m^2 K), a power of a few milliwatts per meter of fiber would be required to heat up the fiber several hundreds of millikelvins. Temperature variations in this range are enough to be dynamically monitored by means of a CP-ΦOTDR system, introduced in the following paragraphs. This model has previously been able to describe the thermal behavior of a copper-coated fiber monitored with a

CP-ΦOTDR while working under experimental conditions similar to the ones here considered [5].

In a CP-ΦOTDR setup, the instantaneous frequency of the probing pulse varies linearly (a linearly *chirped* pulse) [6]. The consecutive Rayleigh *echoes* resulting from these pulses exhibit an accumulative local time shift which is proportional to the variation of the stimulus applied to the fiber at its corresponding point. Hence, by computing the local delay $\delta t(z)$ along the trace with respect to a previous one (reference), this stimulus (namely temperature $\delta T(z)$ or strain $\varepsilon(z)$) can be quantified with every shot. In addition, the performance of this sensor makes easy reaching temperature/strain resolutions in the order of mK/nε. As with conventional ΦOTDR setups, the interrogator update rate is solely limited by the time of flight of the pulses injected, i.e., by the length of the fiber under test. A typical repetition rate for tens of km-long fibers is in the range of several kHz. This makes the CP-ΦOTDR suitable for distributed dynamic refractive index variations measurements where high sensitivity is also needed. The relation between local relative refractive index change ($\Delta n(z)/n$) and the consequent observed time shift can be deduced from these principles, resulting in the following expression [6]:

$$\delta t(z) = \frac{\nu_o}{\delta \nu}\, \tau_p\, \frac{\Delta n(z)}{n}. \quad (4)$$

Here, τ_p represents the duration of the pulses and ν_o and $\delta\nu$ are their central frequency and chirp spectral range, respectively. The thermo-optic coefficient [10],

$$\frac{\Delta n(z)/n}{\Delta T} = 6.92\cdot 10^{-6}\ \mathrm{K}^{-1}, \quad (5)$$

can be applied to obtain the temperature variation (instead of the refractive index change) in terms of the trace delay.

The setup of the employed temperature sensor, in comparison with a conventional ΦOTDR interrogator, requires the additional means to induce the pulse chirp and to perform the traces acquisition at its corresponding bandwidth. The chirp can be easily applied by periodically modulating the bias current of the continuous wave laser source (1550 nm), which is synchronously pulsated before entering the fiber under test (FUT). The 30 ns long pulses generated for this work determine the 3 m spatial resolution of the sensor, which matches the length of the excited fiber region. The power returning from the FUT is conditioned and redirected to a 1 GHz fast p-i-n photodetector. Traces are digitized in a 40 GSa/s oscilloscope (providing a relative refractive index change resolution around 10^{-8} for the applied chirp) and processed in real time by a computer, where refractive index/temperature readouts were registered at a repetition rate of 25 Hz.

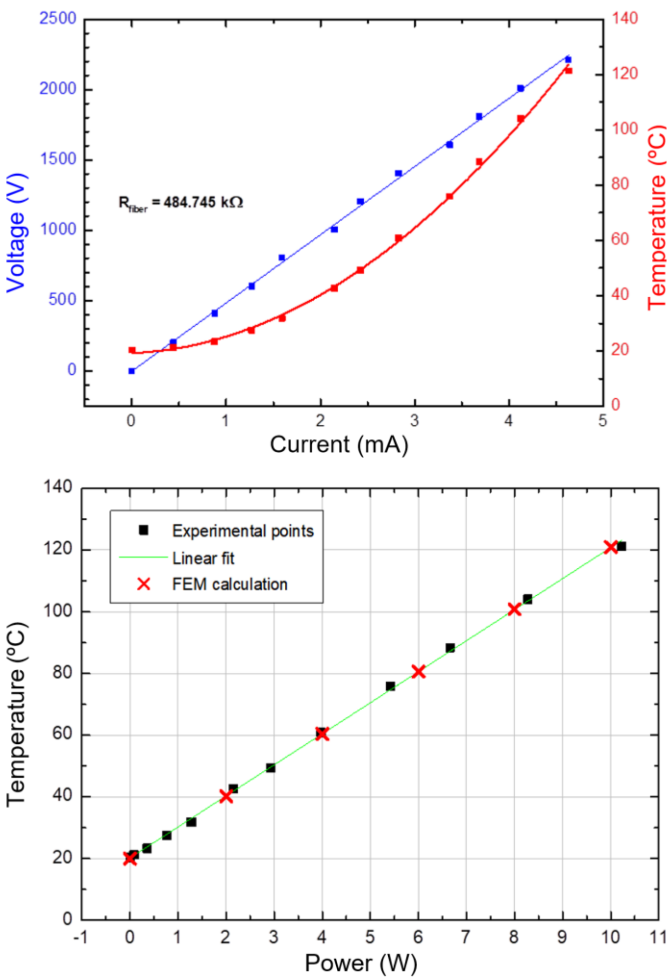

Fig. 3. Current-voltage plot and temperature of C-coated fiber under DC bias (top); The temperature depends linearly on the power applied. At 10 W it exceeds 120ºC (bottom).

III. Numerical and Experimental Results

The possibility of producing a controllable heating in the fiber was first tested. The results guarantee a wide range of temperatures of operation without a noticeable deterioration of the carbon coating, which should keep its hermeticity to small molecules after a current has been applied to it. Figure 3 (top) shows a plot of the ohmic behavior of the carbon film (blue trace) as registered by a commercial Raman DTS sensor for the steady states forced by the DC current. The linear dependence of the current with applied voltage gives a constant resistance of 485 kΩ within this temperature range for the tested piece of fiber. The temperature dependence on current is parabolic, as

Fig. 4. Thermal infrared image of the optical fiber segment employed in the test while DC current produces Joule heating on its carbon coating.

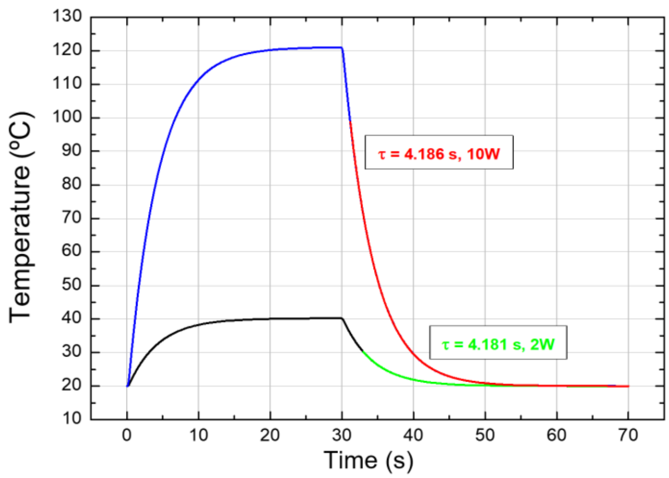

Fig. 5. FEM simulation results considering the geometry, composition and experimental setup of the sample fiber segment under natural convection, h = 25 W/(m^2 K). The theoretical curves correspond to electrical powers of 2 and 10 W, respectively, over 3 m.

expected from an ohmic resistor (red curve). This implies that a plot of the temperature reached as a function of electrical power must show a linear dependence, as observed in Fig. 3 (bottom). The temperature reaches 121ºC for 10 W applied, a remarkable value considering that the carbon layer thickness is only 20 nm. A simulation of the experimental conditions was performed by means of finite element method (FEM) software. For this, a convective efficiency *h* =25 W/(m^2 K) was selected. The resulting steady temperature calculation is also depicted, matching the data, what verifies the model. For comparison, a FLIR IR camera with resolution 100 mK was used (Fig. 4), giving good agreement with the DTS measurements.

Similar conditions were modeled to study the dynamics of the system. Considering the heating and cooling process induced by a square current pulse, the dynamic characteristic constant of the system (τ) was estimated by fitting the temperature evolution to the exponential expression in Eq. 2. Figure 5 shows two examples of the temperature evolution under the switching current (corresponding to both ends of the line in Fig. 3, bottom). The results indicate that this parameter is independent of the applied power in the whole tested range. This is also the behavior expected for the experimental tests. The value obtained for the time constant from the simulation was τ^{sim} = 4.18 s.

The measurements were done on a 3 m length section of single-mode C-coated fiber in this case. A resistance of 1.4 MΩ was measured for this section (~4.7 kΩ/cm). To test this regime the current was applied intermittently at a 100 mHz frequency. This produced a cyclic cooling-heating response for a set of different dissipated power linear densities (all of them below ~12 mW/m). In Fig. 6 (top) the results acquired with the CP-ΦOTDR interrogator are plotted. We can observe that the actual refractive index oscillations typically tracked during the heating cycles exhibit a repeating exponential pattern like the one shown in Fig. 5. The curve chosen corresponds to the smallest heating power density employed in these tests

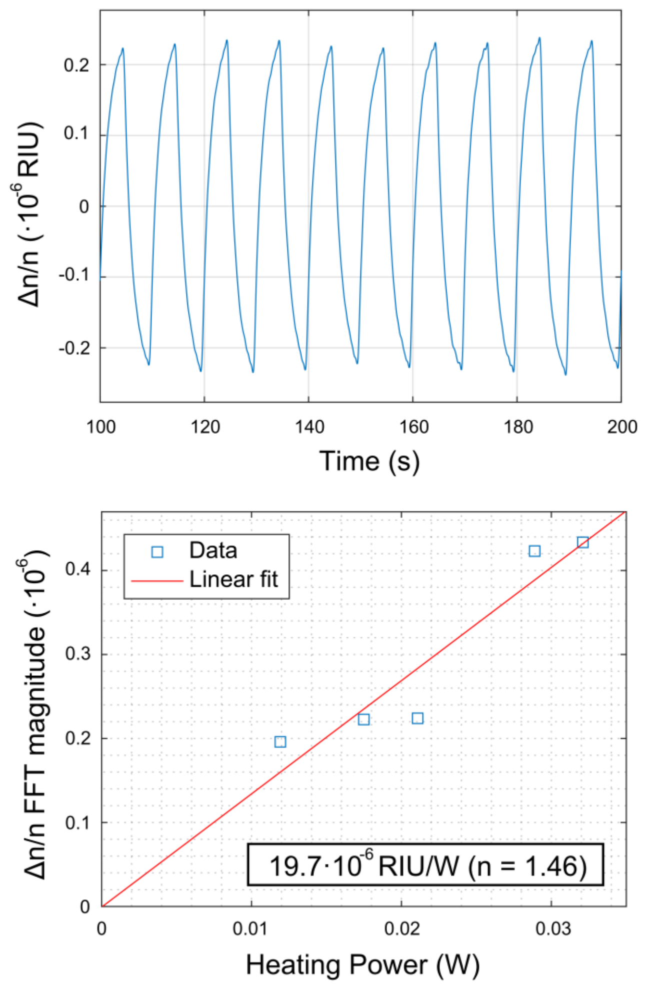

Fig. 6. Top: typical relative refractive index variation cycles induced by a 4 mW/m dissipated power; Bottom: cycles peak amplitude for different values of applied Joule power.

(4 mW/m). The data obtained for each given dissipated power value was analyzed in time but also in the frequency-domain, allowing to perform a high-pass filtering of the signal. This procedure is followed in order to discard slow room temperature or laser frequency drifts. The amplitude of the variations was also measured in the frequency-domain, providing an average of all the cycles registered corresponding to a same dissipated power value. These amplitudes are represented in terms of refractive index change in correlation with the power applied to the FUT in Fig. 6 (bottom). The presented linear fit provides the characteristic sensitivity of the carbon-coated fiber sample in terms of relative refractive index units (RIU): 19.7·10^{-6} RIU/W (for a standard single-mode fiber with n~1.46 around 1550 nm).

The time-domain signal was chopped in order to average all the cycles obtained for each dissipated power. An example is shown in Fig. 5, corresponding to a power density of 4 mW/m. An exponential fitting was performed over the resulting averaged curves in order to obtain the characteristic time parameter τ for the coated fiber. The average and standard deviation of the values experimentally obtained for the system was $\langle\tau^{exp}\rangle$ = (1.7±0.1) s. This final result shows good agreement

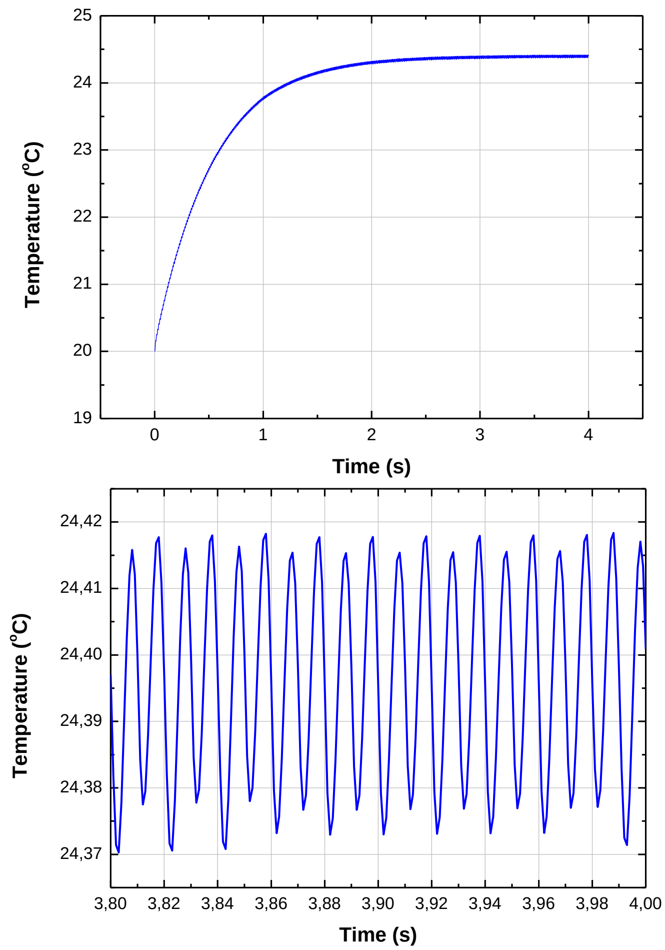

Fig. 7. Top: Fiber under AC thermal excitation, taking ~3 seconds to reach the steady operation temperature (corresponding to an AC effective power density of 1 W/m); Bottom: detail of the temperature modulation once the operation point has been reached.

with the FEM simulations in order of magnitude of τ. However, we must remark the variability implicit in the model, as some theoretical parameters, such as the convective efficiency h, are not easy to estimate or control in the experimental setup.

Owing to the thermal nature of the driving mechanism, the behavior theoretically predicted and experimentally verified may seem too slow for the proposed application. Such time constants would restrict the device to systems working in frequency ranges of several hertzs. However, it is possible to take advantage of the initial, fast refractive index variation shown in Fig. 5 and Fig. 6 (top) when the current is switched on or off. If the available voltage source can provide enough current, this method will easily introduce any phase shift in a few milliseconds, allowing for operation frequencies in the order of ~100 Hz.

A simulation of the response to a 50 Hz AC signal of just 1 W/m is also shown in Fig. 7 (top). A few seconds after the current has been switched on, the steady operating point is reached. Figure 7 (bottom) shows the detail of the temperature modulation, which corresponds to a phase modulation of amplitude around π rad. By applying an adequate driving current, the operating bandwidth of the system can be

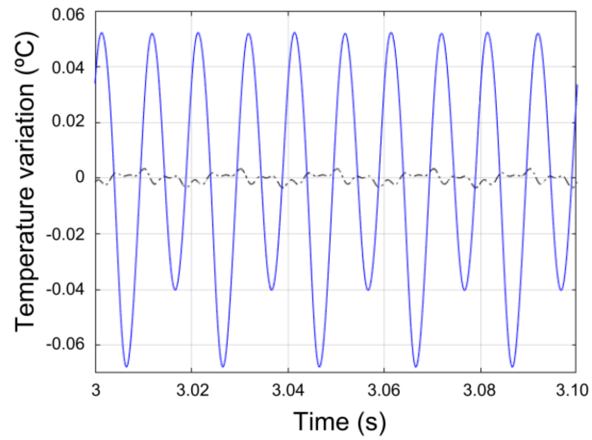

Fig. 8. Experimental steady heating for 1 W/m at 50 Hz (blue, solid), compared to the cold state (black, dashed).

effectively extended. This regime was also experimentally tested. Figure 8 shows the response of the fiber to the same power density and under similar conditions. Both heated (blue, solid) and non-excited (black, dashed) steady states are shown (after filtering out noise) to discard the modulation is due to electrical influence on the sensing system. This demonstrates that, under the right conditions, a modulation of 50 Hz in the C-coated fiber is possible. Note that the variations in the amplitude of the sinusoidal signal shown in Fig. 8 are not the result of a non-linear operation of the distributed temperature sensor, but a thermal consequence of the strong first harmonic (100 Hz) presence in the power supply signal.

According to equation (3), another strategy could be taken to enhance the dynamic response. As τ depends on h, further experiments and simulations were done with the coated fiber immersed in an external flow. However, the forced convection contribution (tested for both air and water as coolants) showed no relevant impact on the time constant, indicating the response of the fiber is determined by the thermal properties of silica and acrylic rather than the coolant. This could happen if thermal conduction in the acrylate wall sets the heat transport bottleneck in the system. Such hypothesis is consistent with the fact that the conductive efficiency of acrylate (which is included in C^{eff} in Eq. 3) is lower than the convective efficiency h of water. Hence, the main temperature drop will develop in the acrylate layer. On the other hand, implementing such a cooling system would add extra complexity to the device.

IV. Conclusion

In this work the viability of an all-fiber phase modulator which is based on the Joule effect to control the refractive index change in a carbon-coated fiber is tested as a proof of concept and continuation of our previous work [11]. As aforementioned, other conductive materials, such as a metal coating, could provide the same control mechanism as demonstrated in reference [5], and a similar hermeticity [3], but presenting other important disadvantages for certain applications (higher weight and lower miniaturizability).

We demonstrate that the heating method can provide temperatures well above 100ºC thanks to Joule effect on a thin carbon layer, and we present a study of the electrical behavior and the dynamics of the heating process. According to experimental results and model, refractive index modulations in the frequency range of 100 Hz could be easily achieved with a simple implementation.

REFERENCES

[1] G. A. Brown and A. Hartog, "Optical fiber sensors in upstream oil & gas," *J. Petrol. Technol.*, vol. 54, no. 11, pp. 63-65, 2002.

[2] P. Puangmali, H. Liu, K. Althoefer, and L. D. Seneviratne, "Optical fiber sensor for soft tissue investigation during minimally invasive surgery," presented at *ICRA*, 2008.

[3] P. J. Lemaire and E. A. Lindholm, "Hermetic optical Fibers: Carbon-Coated Fibers," in *Specialty optical fibers handbook*, A. Méndez, and T. F. Morse eds., Academic Press, 2007, ch. 14.

[4] H. Bai, and G. Shi, "Gas sensors based on conducting polymers," *Sensors*, vol. 7, no. 3, pp. 267-307, 2007.

[5] A. Garcia-Ruiz, A. Dominguez-Lopez, J. Pastor-Graells, H. F. Martins, S. Martin-Lopez, and M. Gonzalez-Herraez, "Long-range distributed optical fiber hot-wire anemometer based on chirped-pulse ΦOTDR," *Opt. Express*, vol. 26, no. 1, pp. 463-476, Jan., 2018.

[6] J. Pastor-Graells, H. F. Martins, A. Garcia-Ruiz, S. Martin-Lopez, and M. Gonzalez-Herraez, "Single-shot distributed temperature and strain tracking using direct detection phase-sensitive OTDR with chirped pulses," *Opt. Express*, vol. 24, no. 12, pp. 13121-13133, Jun., 2016.

[7] A. Sudirman, L. Norin, and W. Margulis, "Increased sensitivity in fiber-based spectroscopy using carbon-coated fiber", *Opt. Express*, vol. 20, no. 27, pp. 28049–28055, 2012.

[8] A. A. Stolov, J. J. Lombardo, B. E. Slyman, J. Li, W. K.S. Chiu, "Carbon coatings on silica glass optical fibers studied by reflectance Fourier-transform infrared spectroscopy and focused ion beam scanning electron microscopy," *Thin Solid Films*, vol. 520, no. 13, pp. 4242-4248, 2012.

[9] T. L. Bergman, A. S. Lavine, F. P. Incropera, and D. P. DeWitt, "Introduction to convection," in *Fundamentals of heat and mass transfer*, John Wiley & Sons, 2011, ch. 6.

[10] Y. Koyamada, M. Imahama, K. Kubota, and K. Hogari, "Fiber-optic distributed strain and temperature sensing with very high measurand resolution over long range using coherent OTDR," *J. Lightw. Technol.*, vol. 27, no. 9, pp. 1142–1146, May, 2009.

[11] A. Garcia-Ruiz, H.F. Martins, R. Magalhães, J.M. Pereira, O. Tarasenko, L. Norin, W Margulis, S Martin-Lopez, and M. Gonzalez-Herraez, "Hermetic All-Fiber Phase Modulators Using Joule Heating in Carbon-Coated Fibers," in *Proc. 26th Optical Fiber Sensors*, 2018, p. WD4.